© 2017 IJSRST | Volume 3 | Issue 8 | Print ISSN: 2395-6011 | Online ISSN: 2395-602X
Themed Section: Science and Technology

# Preparation and Characterisation of Pure and Zn-doped $SnO_2$ Nanoparticles

**K. Sujatha[1*], T. Seethalakshmi [2]**

[1] Assistant Professor, PG Department of Physics, Vellalar College for Women,Thindal, Tamilnadu, India
[2] Assistant Professor, PG Department of Physics, Karur Government College, Karur, Tamilnadu, India.

## ABSTRACT

In this report,Pure and Zn- doped SnO2 nano powders were synthesized by co-precipitation method. The structure, surface morphology, optical, and functional groups were analyzed by X- ray diffraction, Field Emission Scanning Electron Microscope(FESEM), UV-Vis spectroscopy, Fourier transform infrared spectroscopy (FTIR), photoluminescence spectra, Energy Dispersive Spectroscopy(EDAX) and cyclic voltammetric method, respectively. The results were compared with pure tin oxide nanoparticle. X-ray analysis shows that the obtained power has tetragonal rutile type structure with average crystallite size of 34 nm which reduced to 9 nm with Zn addition. Increase in band gap is observed from UV-Vis spectroscopy by the addition of zinc in SnO2. PL spectrum of the pure and doped samples detected two strong emission peaks at 437nm, 465nm due to the surface defect and oxygen vacancies in SnO2 nanoparticles. The electrochemical nature of the samples has been studied using cyclic voltammetric method.Thus the co-precipitation method is convenient, easy, simple, low cost and effective synthesis of nanoparticles.

**Keywords:** SnO2, Zn doping, FESEM, Optical Properties; Co-Precipitation Method.

## I. INTRODUCTION

Nano structured metal oxides have attracted an extensive research interest due to their unique electrical, physical, chemical and magnetic properties as well as their potential for technological applications[1]. Tin oxide ($SnO_2$) is a potential n-type semiconductor with a wide band gap of 3.63 eV, has been widely investigated in battery materials[2], transistors opto-electronic devices[3] and gas sensors[4]. To improve the performance of $SnO_2$, a fashionable way is doping $SnO_2$ with proper metal elements.Many methods have been adopted for synthesis of $SnO_2$ Such as sol-gel[5,6&7], Combustion route[8,9&10],hydrothermal[11 &12,] Microwave synthesis [13, 14 &15],chemical vapour deposition[16],spray pyrolysis[17] and thermal evaporation of oxide powders[18]., Conductive oxides are the capable materials for the fabrication of transparent electronics and optoelectronic devices in the ultraviolet (UV) region because of their wide band gap and high mobility.

In the above techniques, co-precipitation is a attractive method due to its short preparation time, low cost, high purity, homogeneous distribution of doping element and also the ability to yield excellent polycrystalline samples. However, the SnO2 original crystal structure can change as well with the dopant nature.

In the present work, pure and Zn doped $SnO_2$ powder was synthesized using co-precipitation method. The advantage of coprecipitation is the good reproducibility and low temperature is required to obtain the compound, which can limit the formation of large grains. Zinc is a quite active element. It dissolves in both acids and alkalis. In the final product $Zn^{2+}$is therefore expected to replace $Sn^{4+}$ in the $SnO_2$ matrix, which increase the conductivity and the possibility to a variation of the band gap value. The prepared materials were analyzed using structural and optical techniques. The structural and optical properties of the nanoparticles were investigated in detail.

## II. EXPERIMENTAL PROCEDURE

### 2.1 Chemicals

The tin chloride ( $SnCl_4.5H_2O$ Merck, Germany) and zinc chloride (hydrous $ZnCl_2.6H_2O$ Merck, Germany) have been used as starting material for the synthesis of Zn-doped tin oxide nanoparticles by co-precipitation method.

### 2.2 Preparation of $SnO_2$ Powder

In a typical experimental procedure, 4 g tin (II) tetrachloride was dissolved in 200ml distilled water under vigorous stirring for 20 minutes. Aqueous ammonia was added drop wise to the resulting solution in order to modulate the pH at 12. The solution was then left for constant stirring for about 30 minutes. The precipitate was collected and washed with de-ionized water. After drying at 100ºC in oven for 24 hours, the $SnO_2$ nano particles was obtained .In order to improve the crystanality, it was further annealed at 500ºC for 2 hours in furnace in ambient atmosphere .

### 2.3 Preparation of Zn doped $SnO_2$ Powder

For preparation of Zn- doped $SnO_2$ nano powder, 1g $ZnCl_2$ was added to the pH balanced solution and the mixture was stirred for 30 minutes. The procedure adopted to produce nano structured pure $SnO_2$ was used to obtain Zn doped nano $SnO_2$ powder.

## III. CHARACTERIZATION TECHNIQUES

Pure & Zn dope SnO2 nanopowders were successfully characterized by the following techniques.The average crystalline size and structure was analysed by using powder X-ray diffraction Bruker Diffractometer within the range from 10° to 80° using CuKβ as X-ray source. The Scanning Electron Microscopy MODEL PHILIPS XL-30 was used to observe morphology of the prepared nanoparticles and elemental identification of nanoparticles were done by EDAX. The optical parameters of the samples were measured by UV-VIS-NIR spectrophotometer (USB 4000, Ocean Optics-USA). The functional groups were analyzed by using FTIR spectroscopy (Perkin-Elmer System 2000). The PL spectra of pure and Zn doped SnO2 were registered using SL 174 spectroflurometer. Cyclic voltammetric (CV) experiments were performed with a Versa STAT MC electrochemical analyzer, in single compartmental cells using tetrabutylammonium perchlorate as a supporting electrolyte. The electrochemical behavior of pure and Zn doped SnO2 in the potential range +1.5to -2.0 V were recorded.

## IV. RESULTS AND DISCUSSION

### 4.1 X-Ray Diffraction Analysis

Non-destructive X-ray diffraction analysis is a useful technique to determine the sample purity, structural perfection and average grain size of the samples.Fig1 shows the XRD pattern of pure and Zn doped SnO2 nanopowders.It can be seen that, all the diffraction patterns could be indexed to tetragonal rutile type structure with space group of p42/mnm,and the results are in good agreement with the standard JCPDS Data(41-1445).In Zn-doped sample, there is no peak evidence of Zn, ZnO (or) any secondary phase,which confirms the purity of samples.

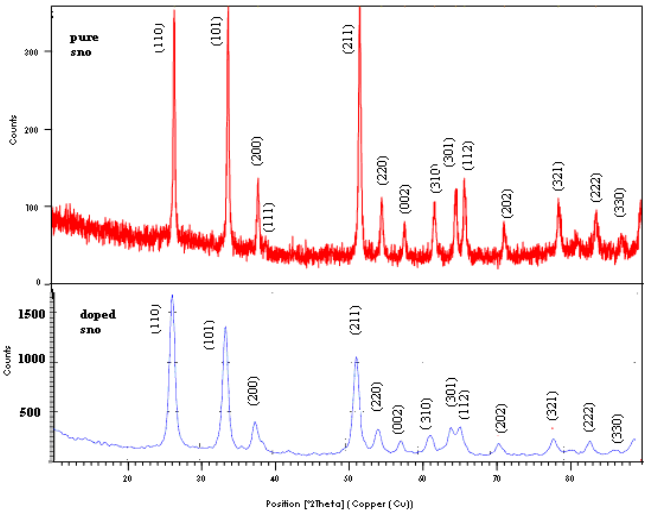


**Figure 1 :** XRD pattern of (a) Pure and b) Zn- doped SnO2 powder

The average crystallite sizes of the nano particles were calculated based on Scherer's equation [19,20].

$$D = \frac{K\lambda}{\beta COS\theta}$$

Where, D is the mean crystallite size, K is the shape factor taken as 0.89, λ is the wavelength of the incident beam, β is the full width at half maximum and θ is the Bragg angle.

$$2d_{hkl} \sin(\theta) = m\lambda$$

Where d is the spacing between the planes in the atomic lattice. h, k, and l are all integers, (hkl) is the lattice

plane index, a and c are lattice constants, $d_{hkl}$ is the distance between two consecutive planes (m=1) with plane index (hkl).

The Dislocation density is calculated by:

$$\delta = 1/D^2$$

The Micro strain is calculated by using the equation:

$$s = \frac{d}{D\sqrt{12}}$$

Where, d is inter planar spacing and D is the crystalline size [21, 22]

The obtained rutile structure was compared with JCPDS data (Card No. 41-1445). The pure $SnO_2$ sample shows 3 major peaks appear at 26.5836°, 33.8611°, and 51.7775°, respectively. Zn doped $SnO_2$ sample reveal small shift in diffraction peaks. Thus the crystallite size of pure and Zn doped SnO2 was 34 ± 1 nm, 9 ± 1 nm respectively.

**Table 1.** XRD Parameters and Size of Particles

| Sample | 2θ (deg) | d-spacing (Aº) | FWHM (deg) | Crystallite size(D)(nm) | Dislocation density (δ) x $10^{15}$ | Micro Strain (S) x $10^{-3}$ |
|---|---|---|---|---|---|---|
| Pure $Sno_2$ | 26.5836<br>33.8611<br>51.7775 | 3.35321<br>2.64734<br>1.76567 | 0.2342<br>0.2342<br>0.3346 | 34.8420<br>35.4466<br>26.3824 | 0.8237<br>0.7959<br>0.1437 | 0.9945<br>0.9774<br>1.3133 |
| Zn doped $Sno_2$ | 26.2291<br>33.5268<br>51.4779 | 3.39491<br>2.67076<br>1.77377 | 0.85220<br>0.83680<br>0.93120 | 9.5686<br>9.9118<br>9.4676 | 1.092<br>1.018<br>1.116 | 3.6212<br>3.4958<br>3.6598 |

When zinc was added to $SnO_2$, then FWHM of diffraction peak was increased, as a result the particle size was decreased to 9 nm. It has been found that the size of pure tin oxide is greater than Zn- doped $SnO_2$. Rozati et al [23] have obtained a decrease in crystallite size when Zn was doped with $SnO_2$ specimen. The XRD pattern of zinc doped $SnO_2$ does not exhibit any additional peak indicating the purity of product. Interplanar distances, dislocation density and the microstrain on the grains were calculated. Dislocation density and microstrain developed in pure and Zn doped $SnO_2$ which can be visualized from the line shifting in the XRD spectra. The lattice constants were calculated from the equation of tetragonal system using the method of least squares [24].

$$\frac{1}{d^2} = \frac{h^2+k^2}{a^2} + \frac{l^2}{c^2}$$

**Table 2.** Structural Parameters

| Sample | Hkl | d-spacing (Aº) | Parameters |
|---|---|---|---|
| JCPDS [41-1445] | 110<br>101<br>211 | 3.3470<br>2.6427<br>1.7641 | a =4.7382Aº<br>c = 3.1871 Aº |
| Pure $SnO_2$ | 110<br>101<br>211 | 3.35321<br>2.64734<br>1.76567 | a =4.7422Aº<br>c= 3.1908 Aº |
| Zn doped $SnO_2$ | 110<br>101<br>211 | 3.39491<br>2.67076<br>1.77377 | a =4.80Aº<br>c= 3.2139 Aº |

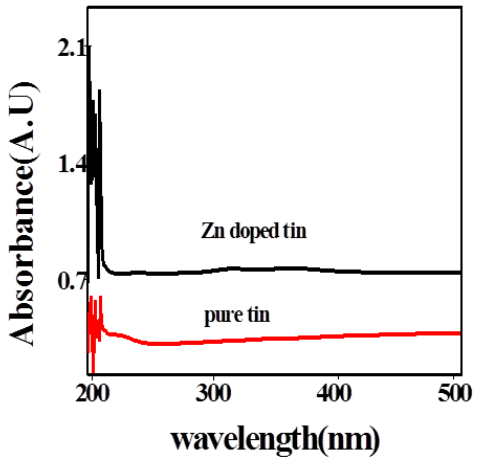


**Figure 2.** UV/Vis/NIR absorption spectra with **pure and Zn doped $SnO_2$ nanoparticles**

From Table 2, the calculated values of lattice parameters 'a' and 'c' are well matched with JCPDS [41-1445].

4.2 Optical properties of pure and Zinc doped SnO2 nanoparticles

UV/Vis/NIR absorption spectra of samples were recorded at room temperature with a wave length range from 200 to 1200 nm. Fig .2 shows the optical absorption spectra of the pure SnO2 nanoparticles.

The UV–vis absorption spectra of pure and Zn doped $SnO_2$ nanoparticles were analyzed and the result was displayed in figure 2 and 3. Both cases, the absorption bands exhibited in the ultraviolet wavelength region which is near the visible-light range.

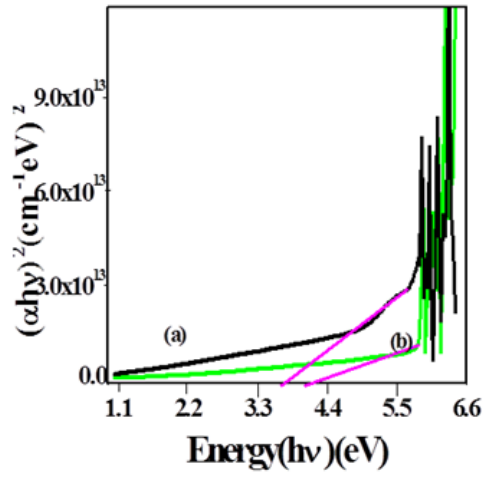


**Figure 3 :** ( αhν ) 2 versus hν plot for (a) Pure and b) Zn- doped SnO2 powder

Using Tauc Plot 25, the band gap was found to increase in Zn doped SnO2 from 3.5 eV (pure SnO2) to 3.9 eV by linear fitting, the absorption band edge in the plot of (αhν) 2 versus hν plot. The increase in band gap might have resulted from the reduced particle size which is a common result due to quantum size effect 26, 27 & 28.

4.3 SEM with EDAX Analysis

Scanning electron microscope was used to observe the surface morphology and average particle size of nanoparticles. Fig. 4 shows the SEM images of pure and Zn- doped SnO2 nanoparticles. In Fig. 4 (a), pure SnO2 nanopowder is very clear which consists of fine tiny nanoparticles and the surface of the nanoparticle is approximately homogeneous with some agglomerates. In Fig. 4(b). In Zn- doped SnO2 nanoparticles, unique surface morphology is observed which consist of globules agglomeration The Zn dopant does not change with the morphology of SnO2, But the average particle size was found to be 32 and 10 nm for pure and Zn-doped SnO2 nanoparticles respectively,which is good agreement with the crystalline size calculated by XRD method23,29.Fig 5 show the EDS spectral of pure and Zn- doped SnO2 nanoparticles. The sample mainly consists of Sn,O and Zn elements.This result confirms the Zn has partially substituted in the SnO2 host lattice site. The composition of Sn is 82.52wt%. O is 12.68wt% and Zn is 4.8wt% in Zn - doped SnO2.

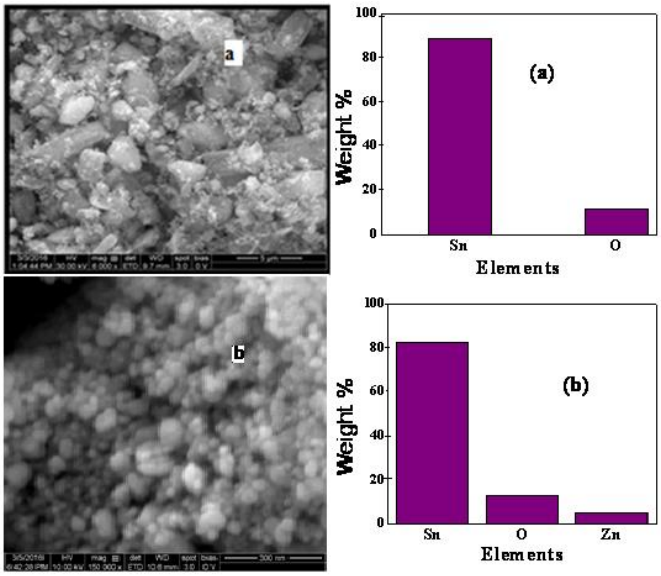


**Figure 4 :** SEM and EDAX images for (a) Pure and (b) Zn- doped SnO2 powder

### 4.4 FTIR Analysis of Pure and Zinc Doped Tin Oxide Nanoparticle

An FTIR spectrum of pure SnO2 nanoparticles was shown in Fig. 5(a). The spectrum of tin oxide exhibited the main characteristic peak at 1743.66, 1551.26, 633.62 and 542.46cm-1as reported previously by Orel et al30. The strong broad peak centered at 633.62 cm-1 corresponds to Sn-O-Sn stretching vibration.

The peak around 1400 cm-1 was assigned to NH stretching vibration from decomposition of NH3. The bands at around 600 and 550 cm-1 were attributed to Sn-O stretching modes of Sn-O-Sn and Sn-OH respectively31. The peaks in the FTIR spectrum at about 3300-3400 and 1645-1620 were due to stretching vibrations of water molecules absorbed at the surface of the tin oxide.

In Zn doped SnO2 samples,a small shifts

was observed. The spectrum of Zn doped SnO2 exhibited the main characteristic peak at 1743.66, 1550.30, 624.94 and 567.08 cm-1 respectively. The strong and broad peak centered at 624.94 cm-1 corresponds to Sn-O-Sn stretching. The broad band between 750 cm-1 and 500 cm-1 was due to the vibrations of Sn-O. From the Fig.5 tin oxide nanoparticles causes some observable changes in the spectrum. Fourier transform infrared spectroscope confirms that the presence of functional groups and also the interaction between the tin oxide and zinc nanoparticles and their corresponding assignments were tabulated in the table 3.

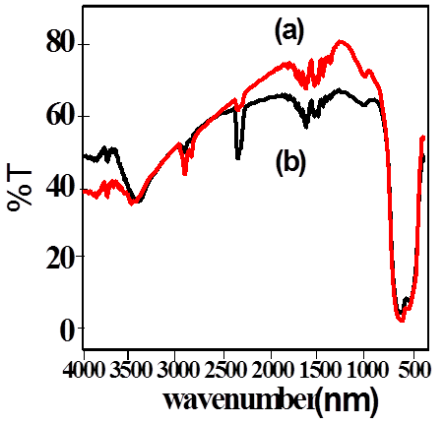


**Figure 5 :** FTIR spectra of (a) Pure and (b) Zn -doped SnO2 nanoparticles

**Table 3.** FTIR ANALYSIS

| Sample | O-H Stretching vibration | O-Sn-O stretching | Sn-O Stretching | NH Stretching Vibration | Sn=O stretching |
|---|---|---|---|---|---|
| **Pure $SnO_2$** | 3431.39<br>1642.88 | 633.62 | 542.48 | 1469.77 | 1028.58 |
| **Zn doped $SnO_2$** | 3492.15<br>1647.70 | 624.94 | 567.08 | 1462.05<br>1380.56 | 1022.28 |

Table 3 gives the value of FTIR peaks and their assignments of SnO2 and Zn doped SnO2 nanoparticles.

### 4.5 Photoluminescence Spectra

The optical properties, surface defects of samples were examined by photoluminescence (PL) spectroscopy using He-Cd laser at room temperature.

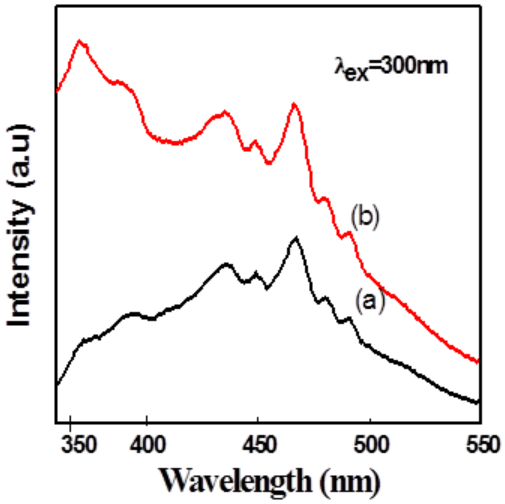


**Figure 6 :** Photoluminescence Spectra of (a) Pure and (b) Zn -Doped SnO2 Nanoparticles

PL spectrum was measured with excitation wavelength of 300nm. Figure 6(a) shows PL spectrum of pure sample detected two strong emission peaks at 437nm, 465nm due to the surface defect and oxygen vacancies which act as luminescent centres in SnO2 nanoparticles32. The intensity of emission peak may vary based on sample's particle size. When the particle size of Zn -doped SnO2 decreases, the intensity of emission may increased due to the particles higher surface –to- volume ratio 25.Compared with pure SnO2 luminescence , Zn -doped SnO2 Figure 6(b) having an additional peak at 372nm. From this observation, it was found that the property of the doped sample was varied compared to the pure sample. Both samples have an emission centre at 437nm & 465nm pointed blue and green light emission. This result suggests that Zn -doped SnO2 samples may find possible potential application in optoelectronic devices.

### 4.6 Cyclic voltammetric (CV) measurement

Figure 7 shows the cyclic voltammogram studies of pure and Zn doped SnO2 nanopowders. The electrochemical parameters of cathodic peak potential

(Epc) and anodic peak potential (Epa) were measured. Both the pure and Zn doped SnO2 samples show irreversible oxidation only (cathodic peak 1.42 V) and reversible reduction anodic peak (-0.5 V) and cathodic (-0.9 V) peak.

The reduction peaks are found to be quasi-reversible in nature with peak - to- peak separation value (ΔEp is 400 mV). Based on this result, it can be concluded that both the samples possesses electrochemical behavior. The cyclic voltammogram shows that the peak positions of pure and Zn doped sample is the same, but the Zn doped sample the peak intensity is increased. This implies that the reduced metallic Zn enhances the good electrochemical behavior when compared to that of pure SnO2.

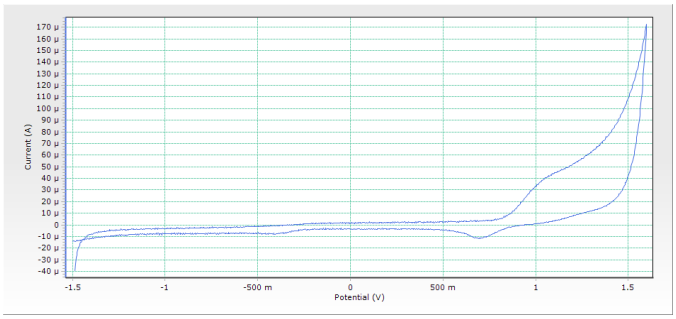


(a)

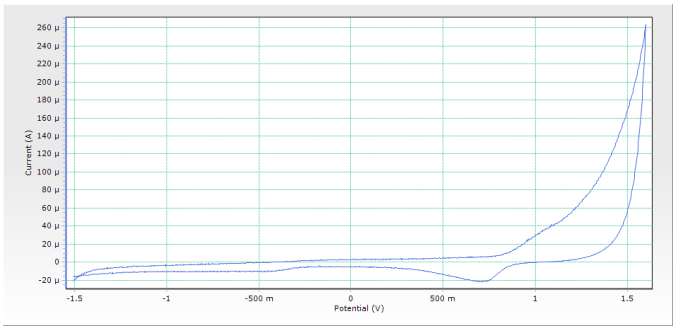


(b)

**Figure 7 :** Cyclic voltammogram of (a) Pure and (b) Zn - Doped SnO2 Nanoparticles

## V. CONCLUSION

In summary, pure and Zn- doped $SnO_2$ nanopowders with tetragonal phase were synthesized by co-precipitation method. The XRD patterns exhibited the rutile type tetragonal structure of pure and zinc doped samples and no impurity phase was observed in XRD. The crystallite size of pure tin oxide was 34 ± 1 nm and zinc doped tin oxide was 9 ± 1 nm. Surface morphology of nano particles showed fine tiny nanoparticles with certain agglomeration. The optical properties were studied using UV-Vis spectroscopy which suggested the band gap is found to vary from 3.5 eV to 3.9 eV with doping. The Photoluminescence study exhibit an increase in the luminescent emission with the decrease in particle size. Thus, the structural, optical properties of

the $SnO_2$ nanoparticles may be changed by doping with Zn. Both samples have an emission centre at 437 nm and 465 nm pointed a blue and green light emission.

## VI. REFERENCES


[1]. Ahn H. J., Choi H. C., Park K. W., Kim S.B., and Sung Y.E., Investigation of the structural and electrochemical properties of size-controlled SnO2 nanoparticles, J. Phys. Chem. B., 108, 9815–9820(2004).

[2]. Chunjoong Kim., Mijung Noh., Myungsuk Choi., Jaephil Cho., Byungwo., and Park., Critical Size of a Nano SnO2 Electrode for Li-Secondary Battery, Chem. Mater. 17, 3297-3301(2005).

[3]. Mayer J. W., Alford T.L., Characterization of the physical and electrical properties of Indium tin oxide on polyethylene napthalate, J.App. Phy. 98, 083705(2005).

[4]. Pinna N., Neri G., Antonietti M., Niederberger M., Nonaqueous Synthesis of Nanocrystalline Semiconducting Metal Oxides for Gas Sensing, Angewandte Chemie International Edition, 43, 4345-4349(2004).

[5]. Brinker C.J., Scherer S. W., Sol–Gel science: the physics and chemistry of sol–gel Processing, Academic Press, New York, (1990).

[6]. Brinker C.J., Bunker B.C., Tallant D.R., Ward K.J., Kirkpatrick R.J., Structure of Sol-Gel Derived Inorganic Polymers: Silicates and Borates, ACS Symposium series, Chapter 26, 360 ,314-332(1988).

[7]. Jones R.W., Fundamental Principles of Sol-Gel Technology, Institute of metals, London (1989).

[8]. Nagaveni K., Hedge M.S., Ravishankar N., Subbanna G.N., Madras G., Synthesis and structure of nanocrystalline TiO2 with lower band gap showing high photocatalytic activity, Langmuir, 20, 2900-2907(2004).

[9]. Nagaveni K., Sivalingam G., Hegde M. S., and Madras G., Solar photocatalytic degradation of dyes: high activity of combustion synthesized nano TiO2 Appl. Catal. B Environ. 48, 83-93(2004).

[10]. Carp O., Huisman C.L., Reller A., Photoinduced reactivity of titanium dioxide, Progress in Solid. State Chemistry, 32, 33–177(2004).

[11]. Chen X., Mao S.S., Titanium dioxide nanomaterials: synthesis, properties, modifications and applications, Chemical Reviews, 107, 2891–2959(2007).

[12]. Yang J., Mei S., Ferreira J. M. F., Hydrothermal synthesis of TiO2 nanopowders from tetraalkylammonium hydroxide peptized sols, Mater. Sci. Eng. C. 15, 183-185(2001).

[13]. Rao K.J., Vaidhyanathan B., Ganguli M., Ramakrishnan P. A., Synthesis of inorganic solids using microwaves, Chem. Mate. 11, 882-895(1999).

[14]. Bhat M. H., Chakravarthy B. P., Ramakrishnan P. A., Levasseur A., Rao K. J., Microwave synthesis of electrode materials for lithium batteries Bull. Mater. Sci. 23, 461(2000).

[15]. Subramanian V., Chen C.L., Chou H.S., Fey G.T.K., Microwave-assisted solid-state synthesis of LiCoO2 and its electrochemical properties as a cathode material for lithium batteries, J. Mater. Chem,11 ,3348-3353. DOI: 10.1039/B105008G (2001).

[16]. Liu, Y., Koep, E., Liu, M.: A highly sensitive and fast-responding SnO2 sensor fabricated by combustion chemical vapor deposition. Chem Mater 17, 3997(2005)

[17]. Paraguay-Delgado, F., Antúnez-Flores, W., Miki-Yoshida, M., Aguilar-Elguezabal, A., Santiago, P., Diaz, R., Ascencio, J.A.: Structural analysis and growing mechanisms for long SnO2 nanorods synthesized by spray pyrolysis. Nanotechnology 16, 688 (2005)

[18]. Dai, Z.R., Gole, J.L., Stout, J.D., Wang, Z.L.: Tin oxide nanowires, nanoribbons, and nanotubes. J. Phys. Chem. B 106, 1274 (2002)

[19]. Parthibavarman M., Hariharan V., Sekar C., High-sensitivity humidity sensor based on SnO2 nanoparticles synthesized by microwave irradiation method, Mater. Sci. Engg. C. 31, 840-844(2011),.

[20]. Krishnakumar T., Jayaprakash R., Nicola Pinna, Singh V.N., Mehta B.R., Phani A. R., Microwave-assisted synthesis and characterization of flower shaped zinc oxide nanostructures,Materials Letters,63 ,242-245(2009).

[21]. Jingran Su Youting Song, Daofan Zhang and Xinan Chang., Characterization of unidirectionally

grown NaCl[sub 1-x]Br[sub x]O[sub 3] crystals, Powder Diffraction, 24 ,234(2009).
[22]. James R Connoly, Introduction to X-ray Diffraction, Spring EPS 400-002(2007).
[23]. Rozati S. M., Shadmani E., Effect of Zn Concentration On Physical Properties of Nanostructure Tin Oxide Films Prepared By Spray Pyrolysis Technique, Dig. J. Nanomate. Biostructures (DJNB) 6 ,365(2011).
[24]. Chou L.J., Cai Y.C., Zhang B., Niu J.Z., Ji S.F., Li S.B., Oxidative coupling of methane over Na-Mn-W/SiO2 catalyst at higher pressure, React. Kinet. Catal.Lett. 76, 311–315(2002).
[25]. Gaidi M., Hajjaji A., Smirani R., Bessais, El Khakni M.A., Structure and photoluminescence of ultrathin films of SnO2 nanoparticles synthesized by means of pulsed laser deposition, J. App. Phys. 108 ,063537(2010).
[26]. Gajendiran J., Rajendran V., Size controlled and optical properties of Zn- doped SnO2 nanoparticles via sol-gel process Optoelectro. & Adv. Mater.Rapid Comm. 5, 44(2011).
[27]. Tan L., Wang L., Wang Y., Hydrothermal synthesis of nanostructures with different morphologies and their optical properties, J. Nanomaterials, 2011, 16(2011).
[28]. Mondal S.P., Ray S.K., Ravichandran J., Manna I., Temperature dependent growth and optical properties of SnO2 nanowires and nanobelts, Bulle. Mate. Sci. 33, 357-364(2010).
[29]. Md Sin N.D., Mamat M. H., Musa M. Z., Abdul Aziz A., Rusop M., Influence of post heat treatment to the properties of ZnO thin film prepared by RF magnetron sputtering, Research and Development (SCOReD), IEEE Student Conference ,88-91(2012).
[30]. K. Anandan, V. Rajendran, J. Phys. Sci. 19, 129 (2014)
[31]. B .Orel,U. Lavvencic-stangar, Z. Crnjakorel, P. Bukorec and M. Kosec, ibid.167(1994)272
[32]. J. Zhang,L. Gao.J.Solid State Chem.177 (2004) 1425-1430
[33]. J. Zhu, Z. Lu, S.T. Aruna, D. Aurbach, A. Gedanken, Chem.Mater. 12, 2557 (2000)